Three-dimensional Radiative Heat Transfer in Glass Cooling Processes

Frank-Thomas Lentes, Schott Glaswerke Mainz (Germany)

Norbert Siedow, Institut für Techno- und Wirtschaftsmathematik e.V., Kaiserslautern (Germany)

Abstract

For the numerical simulation of 3D radiative heat transfer in glasses and glass melts, practically applicable mathematical methods are needed to handle such problems optimal using workstation class computers. Since the exact solution would require super-computer capabilities we concentrate on approximate solutions with a high degree of accuracy. The following approaches are studied: 3D diffusion approximations and 3D ray-tracing methods.

Um den Wärmetransport durch Strahlung in 3D-Geometrie zu beschreiben, werden praktikable mathematische Verfahren benötigt, die es erlauben, solche Probleme auf Computern der Workstation-Klasse optimal zu lösen. Da die volle Lösung der Wärmetransportgleichnung (inklusiv Strahlungswärme) Super-Computer erfordern würde, werden im folgenden Näherungsverfahren vorgestellt, die eine hinreichend genaue Lösung gestatten. Dazu gehören Diffusionsapproximationen und Ray-Tracing in 3D-Geometrie.

1 Introduction

For many industrial applications the modeling of heat transport processes is of utmost importance. This applies especially to radiative heat transfer in semi-transparent materials like glasses. The knowledge of the exact temperature distribution is necessary to control production processes and the final quality of the products. For instance, the temperature distribution during the cooling process of glass influences the internal stress field. Undesired effects like breakage could be the result of a wrong cooling process. In the case of semitransparent materials like glass, heat transfer is not only accomplished by conduction but also by radiation and - when molten - also by convection. This is particularly the case in melting furnaces, during hot processing of glass melts or during the cooling process where radiative heat transfer may dominate over convection and conduction. Conduction and convection are local phenomena. The mean free path for molecular collisions is generally very small. Thermal radiation, on the other side, is generally a global phenomenon. The average distance a photon travels before interacting with a molecule may be very short (e.g. absorption in a metal), but can also be very long (e.g. sun rays). Since the coupling between the energy equation and the equation of radiative transfer is highly nonlinear, it is of great importance to use efficient and accurate solution procedures to the radiation part. In this study we consider a temperature region $\leq 600°$C, where the radiative heat transfer is less or equal to the phononic heat transfer. We concentrate on mathematical approaches for 3D radiative heat transfer with both high computational efficiency and sufficient (and controllable) accuracy, suitable for workstation class computers.

2 Heat Transfer by Conduction and Radiation

Let G be a three-dimensional domain of an absorbing and emitting semitransparent material. The material has a given initial temperature distribution

$$T(\vec{r},0) = T_0(\vec{r}), \;\; \vec{r} \in G. \tag{1}$$

The temperature of the surrounding T_a is known. Then the heat transfer without extra energy sources or heat sinks (exo- or endothermic reactions) in the medium G can be described by the energy equation:

$$c_m \rho_m \frac{\partial T}{\partial t}(\vec{r},t) = \vec{\nabla} \cdot \left(k_h \vec{\nabla} T(\vec{r},t) - \vec{q}(\vec{r},T) \right), \;\; \vec{r} \in G, \;\; 0 < t \leq t^{\star}, \tag{2}$$

where c_m is the specific heat, ρ_m the density, k_h the thermal conductivity, T is the temperature, $\vec{r}$ the position vector, t is the time and $\vec{q}$ the radiative heat flux vector.

Let $\vec{n}$ be the outer normal to the boundary ∂G of the domain G and $\vec{r}_g$ the position vector of a boundary point. The heat flux at the boundary $k_h \frac{\partial T}{\partial \vec{n}}$ is defined by heat convection and diffuse surface radiation (see [1])

$$k_h \frac{\partial T}{\partial \vec{n}} = h(T_a - T) + \varepsilon\pi \int\limits_{opaque} (B(T_a,\nu) - B(T(\vec{r}_g),\nu))d\nu, \; \vec{r}_g \in \partial G, \; 0 < t \leq t^{\star}, \tag{3}$$

where h is the convective heat transfer coefficient, ε the mean hemispheric surface emissivity in the opaque spectral region, $B(T,\nu)$ is the spectral intensity of the black-body radiation given by Planck function in a medium

$$B(T,\nu) = \frac{2 h_p \nu^3 n_g^2}{c_0^2 \left(e^{h_p \nu / k_B T} - 1 \right)}. \tag{4}$$

Here c_0 denotes the speed of radiation propagation in vacuum, the n_g refractive index of glass, h_p Planck's and k_B Boltzmann's constant.

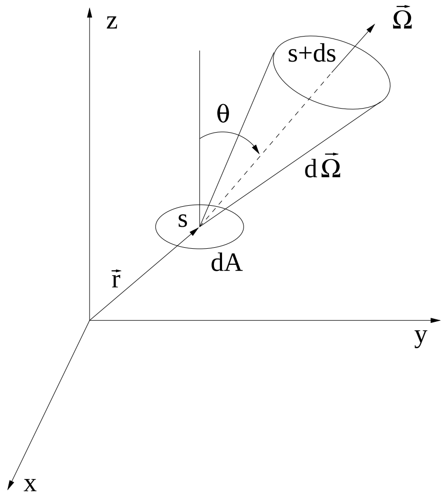

Figure 1: Spectral Intensity

In equation (2) the divergence of the radiative heat flux vector describes the loss of radiation converted in tangible heat. To model the radiative transfer through a semitransparent material like glass we first define the spectral radiative intensity $I(\vec{r}, \vec{\Omega}, \nu)$, as the radiative energy flow per unit solid angle $\vec{\Omega}$, frequency ν and unit area normal to the rays. The solid angle a surface is seen from a certain point is defined as the projection of the surface onto a plane normal to the direction vector, divided by the distance squared (see [2]). Let a beam of radiation of intensity $I(\vec{r}, \vec{\Omega}, \nu)$ travel in the medium in the direction $\vec{\Omega}$ along a path s (see fig. 1). The quantity

$$dI(\vec{r}, \vec{\Omega}, \nu)\, dA\, d\Omega\, d\nu \tag{5}$$

represents the difference in the radiative energy crossing two differential surfaces dA at s and $s + ds$ in the frequency interval $d\nu$, and contained in an element of solid angle $d\Omega$ in the direction $\vec{\Omega}$. The net gain of radiant energy W_r per unit volume dA, per unit solid angle $d\Omega$ and per unit frequency interval $d\nu$ can be written as

$$W_r = \frac{dI}{ds}(\vec{r}, \vec{\Omega}, \nu) = \vec{\Omega} \cdot \vec{\nabla} I(\vec{r}, \vec{\Omega}, \nu). \tag{6}$$

On the other side W_r is composed of those radiant energy changes due to emission and absorption processes within the medium:

$$W_r = W_{emis} - W_{absorp}. \tag{7}$$

The first term W_{emis} represents the gain of radiant energy due to emission. Applying Kirchhoff's law (see [2]) it is given by

$$W_{emis} = \kappa(\nu) B(T, \nu). \tag{8}$$

$\kappa(\nu)$ is the frequency depending extinction coefficient.
The second term in (7) is the loss of radiant energy due to absorption and is proportional to the intensity:

$$W_{absorp} = \kappa(\nu) I(\vec{r}, \vec{\Omega}, \nu). \tag{9}$$

Assuming that the spectral extinction coefficient $\kappa(\nu)$ is piecewise constant with respect to the frequency ν,

$$\kappa(\nu, T) = \kappa_k = \text{const.}, \quad \nu \in [\nu_k, \nu_{k+1}), \quad k = 1, ..., M_k, \tag{10}$$

where M_k is the number of spectral bands, one can introduce the intensity of the k-th spectral band

$$I^{(k)}(\vec{r}, \vec{\Omega}) = \int\limits_{\nu_k}^{\nu_{k+1}} I(\vec{r}, \vec{\Omega}, \nu) d\nu \quad \text{and} \quad B^{(k)}(\vec{r}) = \int\limits_{\nu_k}^{\nu_{k+1}} B(T(\vec{r}), \nu) d\nu. \tag{11}$$

From (6)-(11) the energy balance leads to the radiative transfer equation

$$\vec{\Omega} \cdot \vec{\nabla} I^{(k)}(\vec{r}, \vec{\Omega}) + \kappa_k I^{(k)}(\vec{r}, \vec{\Omega}) = \kappa_k B^{(k)}(\vec{r}). \tag{12}$$

At the boundary we consider transmitting and specular reflecting condition (see fig. 2)

$$I^{(k)}(\vec{r}_g, \vec{\Omega}) = \rho(\vec{\Omega}, \vec{\Omega}') I^{(k)}(\vec{r}_g, \vec{\Omega}') + (1 - \rho(\vec{\Omega}, \vec{\Omega}')) n_g^2 B^{(k)}(T_a). \tag{13}$$

The total radiative heat flux vector $\vec{q}(\vec{r})$ represents the net transport of energy in a given direction $\vec{\Omega}$ per unit area due to radiation from all directions over the unit sphere S^2 and frequency bands and is defined as

$$\vec{q}(\vec{r}) = \sum_{k=1}^{M_k} \int_{S^2} \vec{\Omega} I^{(k)}(\vec{r}, \vec{\Omega}) d\Omega. \tag{14}$$

Using the radiative transfer equation (12) from (14) follows the divergence of the radiative heat flux vector

$$\vec{\nabla} \cdot \vec{q}(\vec{r}) = \sum_{k=1}^{M_k} \kappa_k \left(4\pi B^{(k)}(T(\vec{r})) - \int_{S^2} I^{(k)}(\vec{r}, \vec{\Omega}) d\Omega \right), \tag{15}$$

which describes the power density of the radiative field.

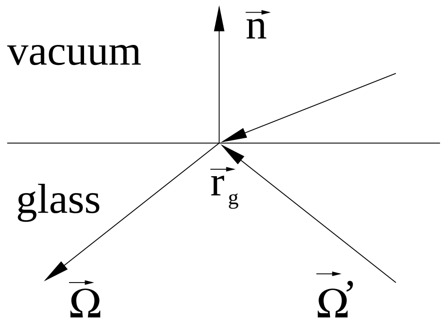

Figure 2. Directions and boundary
of semitransparent medium.

Heat transfer problems by conduction can be solved routinely using commercial software packages. For the calculation of radiative transfer, these packages use only the simplest approximation methods, so that it is not possible to simulate real three-dimensional problems with good accuracy in realistic computing times. Radiative heat transfer in absorbing-emitting media is subject of study for engineers and scientists for many years. The need to determine radiative transfer for many industrial applications is more important than ever before. Due to tight-end quality tolerances of the production the accuracy of the modeling has to be improved significantly.

The intensified interest in the treatment of radiative transfer encouraged the publication of a number of texts devoted to this subject. A comprehensive report about numerical solution methods for radiative heat transfer is given in [2], [3] and especially for semitransparent solids in [4].

Nowadays the method of discrete ordinates is one of the most popular methods which is referred to in literature about the numerical solution of the radiative transfer equation. The main idea of the discrete ordinates method is to transform the equation of radiative transfer into a set of simultaneous partial differential equations. A very simple modification of this method was given long time ago by Schuster (1905) and Schwarzschild (1906) for a one-dimensional, plane-parallel slab. Schuster and Schwarzschild assumed the radiative intensity to be isotropic over the upper and lower hemisphere. So they break up the intensity into two components for two directions. Therefore, the method is commonly referred to as the two-flux method. A generalization of the two-flux method is the discrete ordinates method. The total solid angle of 4π is divided into a set of n discrete directions. A solution to the transport problem is found by solving these n equations of transfer for such a set. Thus, the discrete ordinates method is simply a finite differencing of the directional dependence of the radiative transfer equation. The selection of the discrete ordinates directions is arbitrary. The study of the literature about the selection of discrete ordinates directions shows that it is customary to choose sets of directions and weights that are symmetric (see [5], [6], [7], [8]). Commonly used Level-Symmetric-Quadrature sets can be found in many books about solution methods for the radiative transfer equation, for instance in [2] or [7].

3 An Improved Diffusion Approximation

A very effective class of approximation methods for solving radiative transfer is the class of diffusion approximations. The calculation with these methods is very fast and they can be implemented into commercial software packages easily. One of the first diffusion approximations was developed 1924 by Rosseland (see [9]). A way to derive the Rosseland approximation is to use the formal solution of the radiative transfer equation. Let $\vec{r}_g$ be the boundary point from the point $\vec{r}$ in the direction $-\vec{\Omega}$. From (12) we get

$$I^{(k)}(\vec{r},\vec{\Omega}) = I^{(k)}(\vec{r}_g,\vec{\Omega})e^{-\kappa_k|\vec{r}-\vec{r}_g|} + \kappa_k \int\limits_0^{|\vec{r}-\vec{r}_g|} B^{(k)}(\vec{r}-s\vec{\Omega})e^{-\kappa_k s}ds. \tag{16}$$

The first term on the right hand side is the attenuation of the radiative intensity at the boundary due to the absorption. The second integral term describes the emission along the path between the two points $\vec{r}_g$ and $\vec{r}$ in the direction $\vec{\Omega}$ which is attenuated by absorption coresponding to the distance s to the boundary point $\vec{r}_g$.

Expanding the black-body radiation function $B^{(k)}(\vec{r}-s\vec{\Omega})$ into a Taylor series and substituting this expression into equation (16) leads to

$$\begin{aligned} I^{(k)}(\vec{r},\vec{\Omega}) \;&\approx I^{(k)}(\vec{r}_g,\vec{\Omega})e^{-\kappa_k|\vec{r}-\vec{r}_g|} + B^{(k)}(\vec{r}) - B^{(k)}(\vec{r}_g)e^{-\kappa_k|\vec{r}-\vec{r}_g|} \\ &-\tfrac{1}{\kappa_k}\tfrac{dB^{(k)}}{dT}(\vec{r})\vec{\Omega}\cdot\vec{\nabla}T(\vec{r})\left(1-e^{-\kappa_k|\vec{r}-\vec{r}_g|}\right). \end{aligned} \tag{17}$$

If we assume that the material is optically thick, or $\kappa_k \mid \vec{r}-\vec{r}_g \mid >> 1$, we will get the Rosseland approximation:

$$I^{(k)}(\vec{r},\vec{\Omega}) \approx B^{(k)}(\vec{r}) - \frac{1}{\kappa_k}\frac{dB^{(k)}}{dT}(\vec{r})\vec{\Omega}\cdot\vec{\nabla}T(\vec{r}). \tag{18}$$

Here the radiative intensity is only weakly depending from the solid angle $\vec{\Omega}$. The divergence of the radiative flux vector has the same form as the expression for the conductive heat flux:

$$\vec{\nabla} \cdot \vec{q}^{(k)}(\vec{r}) = -\vec{\nabla} \left(\frac{4\pi}{3\kappa_k} \frac{dB^{(k)}}{dT}(T(\vec{r})) \cdot \vec{\nabla} T \right). \tag{19}$$

Therefore, the Rosseland approximation characterizes the transport of radiation as a diffusion process.

From the numerical point of view the Rosseland approximation is very effective. For each grid point in the discretization scheme of the energy equation (2) a correction k_{rad} (the radiative conductivity) on the thermal conductivity k_h can be added.

On the other side, the limitation to the use of the Rosseland approximation should be recognized. The method is not valid if the medium is optically thin, i.e. if the extinction coefficient κ_k is very small or for points near the boundary. The radiative conductivity k_{rad} can be transformed to

$$k_{rad}(T) = \frac{16 n^2 \sigma}{3 \vec{\kappa}_{Ross}} T^3, \tag{20}$$

where σ denotes the Stefan-Boltzmann constant and $\vec{\kappa}_{Ross}$ is the Rosseland mean extinction coefficient defined by

$$\frac{1}{\vec{\kappa}_{Ross}(T)} = \frac{\int\limits_0^\infty \frac{1}{\kappa(\nu)} \frac{dB(\nu,T)}{dT} d\nu}{\int\limits_0^\infty \frac{dB(\nu,T)}{dT} d\nu}. \tag{21}$$

Since the Rosseland approximation is only asymptotically valid for large (optical) thicknesses, the concept of the active thermal conductivity was developed to handle problems with finite optical depths (see [10]). It is suggested to distinguish between an active and a passive thermal conductivity. The latter is attached to the heat transfer through long-range photons most of which are both emitted and absorbed outside the glass volume, the former to the heat transfer through phonons and short-range photons which have an intense energy exchange with the glass. As the temperature distribution in the glass volume can be influenced only by heat exchange in which the glass is actively involved, it is determined by the active conductivity. The sum of the active and the passive thermal conductivity indicates the overall heat flux through the glass. The corresponding radiative conductivity is always smaller than the Rosseland value and is by its very nature thickness depending.

On the other side for boundary points $\vec{r} = \vec{r}_g$ from (17), follows the identity:

$$I^{(k)}(\vec{r}, \vec{\Omega}) = I^{(k)}(\vec{r}_g, \vec{\Omega}). \tag{22}$$

These two limits, (18) and (22), let us hope that the approximation (17) for the spectral radiative intensity is better than the classical Rosseland approximation (18). Using the boundary condition (13), approximating the reflected spectral intensity at the boundary by the black-body function and applying the definition (14) with the approximation (17) for the divergence of the radiative flux then holds:

$$\begin{aligned} \vec{\nabla} \cdot \vec{q}^{(k)}(\vec{r}) \; &= \kappa_k \int\limits_{S^2} (1 - \rho(\vec{\Omega})) \left(B^{(k)}(T(\vec{r}_g)) - n_g^2 B^{(k)}(T_a) \right) e^{-\kappa_k d(\vec{r}, \vec{\Omega})} d\Omega \\ &\quad - \vec{\nabla} \left(\tfrac{1}{\kappa_k} \tfrac{dB^{(k)}}{dT} (T(\vec{r})) A \cdot \vec{\nabla} T \right), \end{aligned} \tag{23}$$

with $d(\vec{r}, \vec{\Omega}) = \mid \vec{r} - \vec{r}_g \mid$ and a symmetric diffusion tensor A in form of a symmetric 3×3-matrix.

In general this improved diffusion approximation is anisotropic. Assuming that the radiative field is only weakly depending from the direction, A can be replaced by an orthotropic diffusion tensor in form of a diagonal matrix

$$\begin{cases} A(\vec{r}) = \begin{pmatrix} a_1(\vec{r}) & 0 & 0 \\ 0 & a_2(\vec{r}) & 0 \\ 0 & 0 & a_3(\vec{r}) \end{pmatrix}, \qquad \vec{\Omega} = (\Omega_1, \Omega_2, \Omega_3)^T, \\ \\ a_j(\vec{r}) = \int\limits_{S^2} \Omega_j^2 \left(1 - e^{-\kappa_k d(\vec{r},\vec{\Omega})}\right) d\Omega, \qquad j = 1, 2, 3, \end{cases} \tag{24}$$

which can easily be used in a commercial software package.

The second term on the right hand side of (23) represents a correction to the heat conduction due to the radiation. The first term contains the boundary condition and depends from the geometry of the considered domain. For the integration over the solid angle a Level-Symmetric-Quadrature can be used.

Finally the heat transfer equation (2) can be replaced by:

$$\begin{aligned} c_m \rho_m \frac{\partial T}{\partial t}(\vec{r}, t) &= \vec{\nabla} \cdot \left(\left((k_h + \sum_k \frac{1}{\kappa_k} \frac{dB^{(k)}}{dT}(\vec{r}) A \right) \vec{\nabla} T(\vec{r}, t) \right) \\ &- \sum_k \kappa_k \int\limits_{S^2} (1 - \rho(\vec{\Omega})) \left(B^{(k)}(T(\vec{r}_g)) - n_g^2 B^{(k)}(T_a) \right) e^{-\kappa_k d(\vec{r},\vec{\Omega})} d\Omega. \end{aligned} \tag{25}$$

4 A Hybrid Method

Because of the requirement that the solution method should be easily applicable to arbitrary convex three-dimensional solids we used a hybrid model based on the discrete ordinates method, the ray-tracing and the improved diffusion approximation.

First the solid angle 4π is divided into a set of discrete directions.

$$\vec{\Omega}_1, \vec{\Omega}_2, ..., \vec{\Omega}_n. \tag{26}$$

We used level-symmetric sets described in [5]. The left-hand side of the radiative transfer equation (12) can be written as the directional derivative along the path s_i

$$\vec{\Omega}_i \cdot \vec{\nabla} I^{(k)}(\vec{r}, \vec{\Omega}_i) = \frac{dI^{(k)}}{ds_i}(\vec{r}, \vec{\Omega}_i). \tag{27}$$

We solve the radiative transfer equation for each grid point $\vec{r}_j$ coming from the energy equation, for each direction $\vec{\Omega}_i$ and each spectral band k along the path s_i

$$\frac{dI^{(k)}}{ds_i}(\vec{r}_j, \vec{\Omega}_i) + \kappa_k I^{(k)}(\vec{r}_j, \vec{\Omega}_i) = \kappa_k B^{(k)}(\vec{r}_j), \tag{28}$$
$$j = 1, 2, ..., m, \;\; i = 1, 2, ..., n, \;\; k = 1, 2, ..., M_k.$$

The specular reflecting boundary condition leads to the coupling of various directions (see fig. 3), where the reflected directions ($\vec{\Omega}_l$ in figure 3) don't have to be elements of the apriori chosen set of discrete ordinates. Because of this problem and the mentioned requirement that the solution method should be easy to apply to general three-dimensional solids we use a ray-tracing technique.

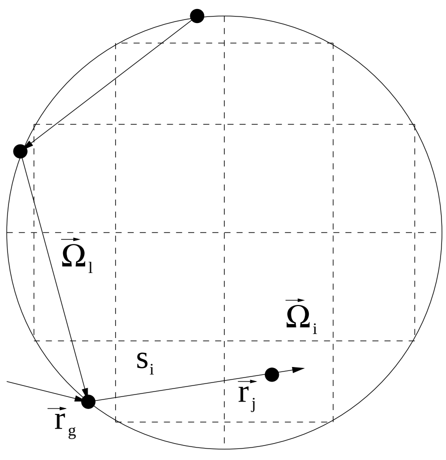

Figure 3. Spatial and directional discretization within disc.

At the boundary $\vec{r}_g$ we have to take into account that the intensity in this point is the sum of the reflected part coming from the direction $\vec{\Omega}_l$ and the part coming from the outside

$$I^{(k)}(\vec{r}_g, \vec{\Omega}_i) = \rho(\vec{\Omega}_i, \vec{\Omega}_l) I^{(k)}(\vec{r}_g, \vec{\Omega}_l) + (1 - \rho(\vec{\Omega}_i, \vec{\Omega}_l)) n_g^2 B^{(k)}(T_a). \qquad (29)$$

The ray-tracing technique is very time consuming. In order to overcome this limitation the domain G is divided into two parts. In a small region near the boundary the ray tracing is applied. For the bigger inner part of G we use the improved diffusion approximation.

5 Some Numerical Results

The above discussed numerical methods were applied to a typical problem of glass manufacturing – to a glass cooling problem.

5.1 Accuracy check for a quasi one-dimensional glass plate

A cylindrical glass plate with radius of 6 cm and height of 0.6 cm (see figure 4) has an initially uniformly distributed temperature of 600°C.

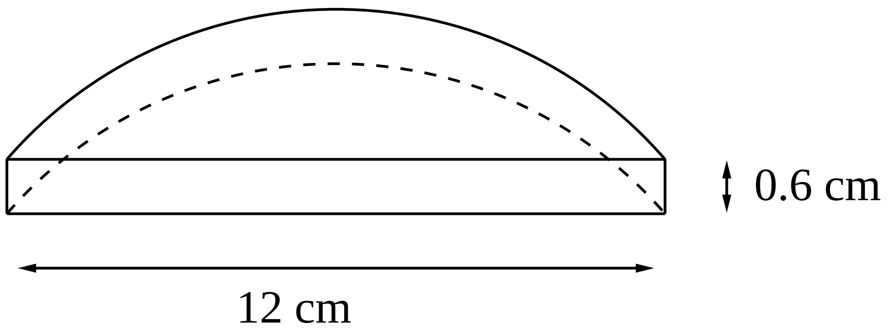

Figure 4. Computational domain.

It cools down through radiation on the boundary surface which is directly exposed to the surrounding temperature of T_a=20°C. Convection heat transfer is neglected, i.e. $h = 0$. We consider 18 frequency bands. The absorption coefficients κ_k are in a range from 10^{-3} until 10^{2} cm^{-1}. The refractive index for glass was chosen to be 1.46.

For the numerical solution of the heat transfer equation a finite difference method with rectangular grid cells, a time step size 0.1s and 48480 spatial grid points was used. The integration over the solid angle was done with an Level-Symmetric-Hybrid ($LSH-8$) method (see [7]).

Figure 5 to 8 show the temperature distributions in the glass plate after 1 and 10 seconds at the axis of symmetry. The temperature along the height in the middle of the cylinder is plotted. The considered cylindrical glass plate is an approximation of the one-dimensional plane-parallel media. Therefore the results of the diffusion approximations are compared with the (exact) one-dimensional solution.

Figure 5 and 6 compare the classical Rosseland approximation with appropriate boundary conditions with the above discussed improved diffusion approximation. After 10 seconds the difference between the exact temperature and the temperature calculated by the Rosseland approximation is greater than 8°C, whereas the temperature calculated by the improved diffusion approximation differs only about 2.5°C.

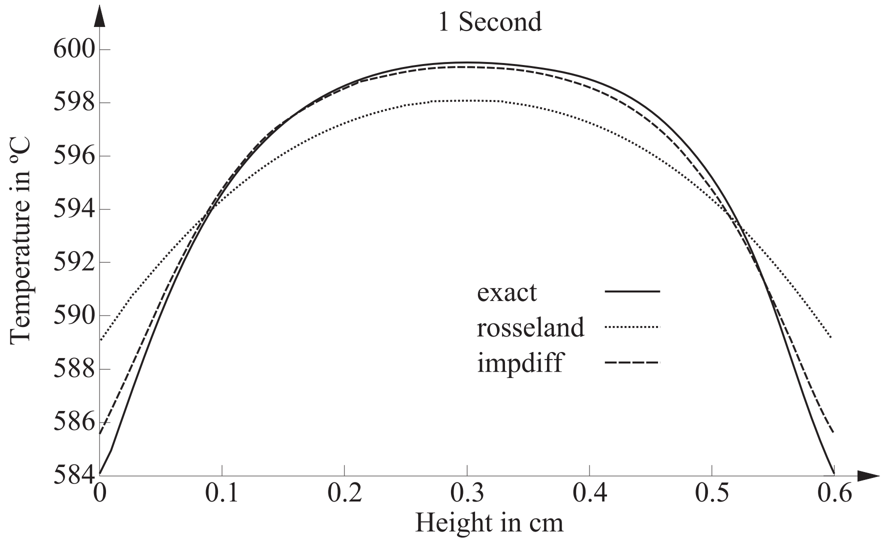

Figure 5. Comparison between the temperatures calculated by the exact, the Rosseland and the improved diffusion approximation method after 1 Second.

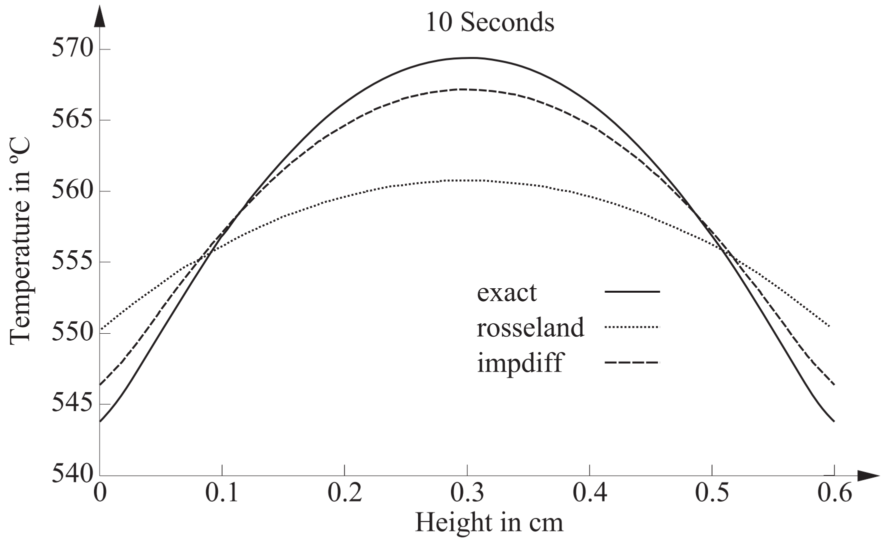

Figure 6. Comparison between the temperatures calculated by the exact, the Rosseland and the improved diffusion approximation method after 10 seconds.

For another calculation the hybrid method was used. In a boundary layer of 0.1 cm the temperature was calculated by a ray-tracing technique. In the remaining part of the cylindrical domain the improved diffusion approximation was used. Figure 7 and 8 show the very good agreement with the exact solution.

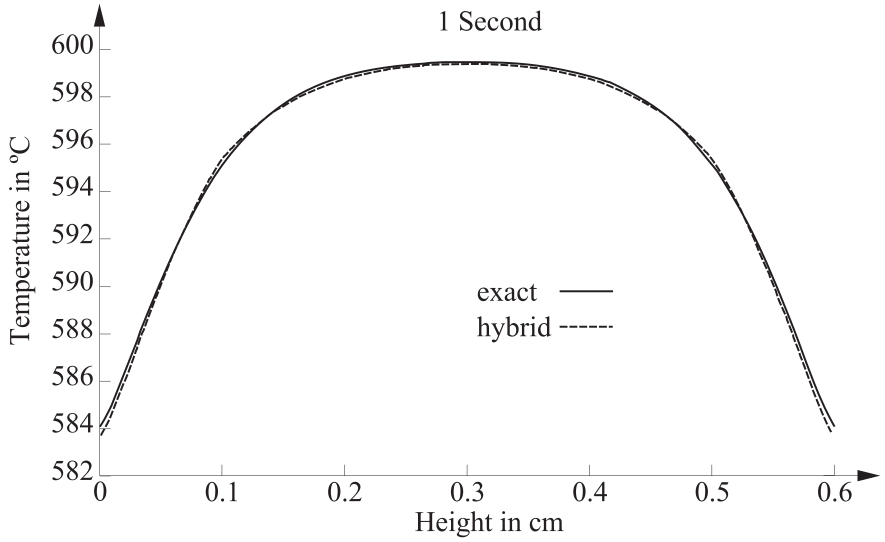

Figure 7. Comparison between the temperatures calculated by the exact and the hybrid method after 1 Second.

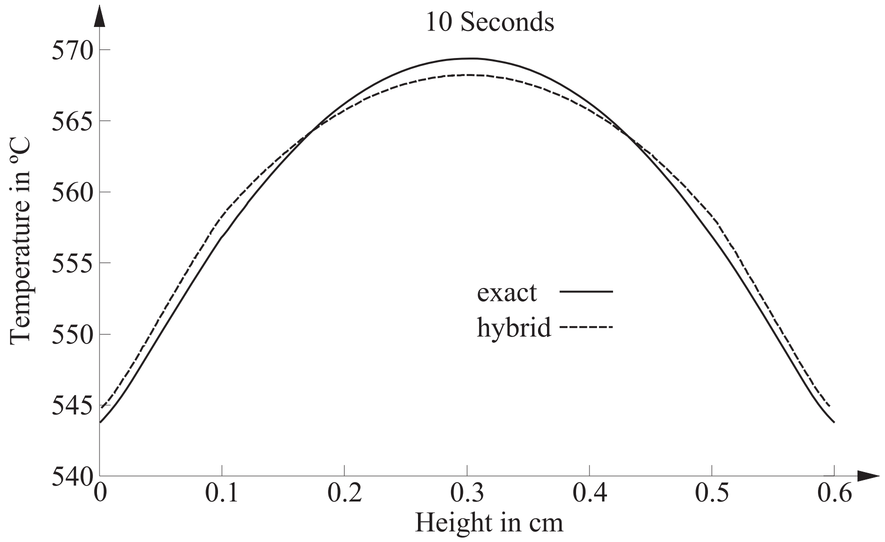

Figure 8. Comparison between the temperatures calculated by the exact and the hybrid method after 10 seconds.

5.2 Comparison of different methods for a three-dimensional example

The second example is a cylindrical glass block with a radius of 1 cm and a height of 2 cm. Consider a horizontal section in the middle of the cylinder. In figure 9 we have plotted the temperature distribution after 10 seconds calculated with different numerical methods: the ray-tracing technique (raytra), the improved diffusion approximation (impdiff), the active thermal conductivity (active) and finally the Rosseland approximation (rosseland). The considered glass block is not optically thick. That's why the Rosseland approximation and the active thermal conductivity give unsatisfactory results. As was described in [10] the concept of active thermal conductivity is preferably valid for one-dimensional problems. Its usage for real three-dimensional problems has no theoretical foundation. While the temperature profile of the Rosseland approximation is too flat, the profile of the active thermal conductivity is too steep. The profile calculated by the improved diffusion method is an acceptable approximation to that calculated by ray-tracing, which is assumed to be very close to the exact solution. It is worth to mention that the improved diffusion approximation can be done as fast as the Rosseland approximation.

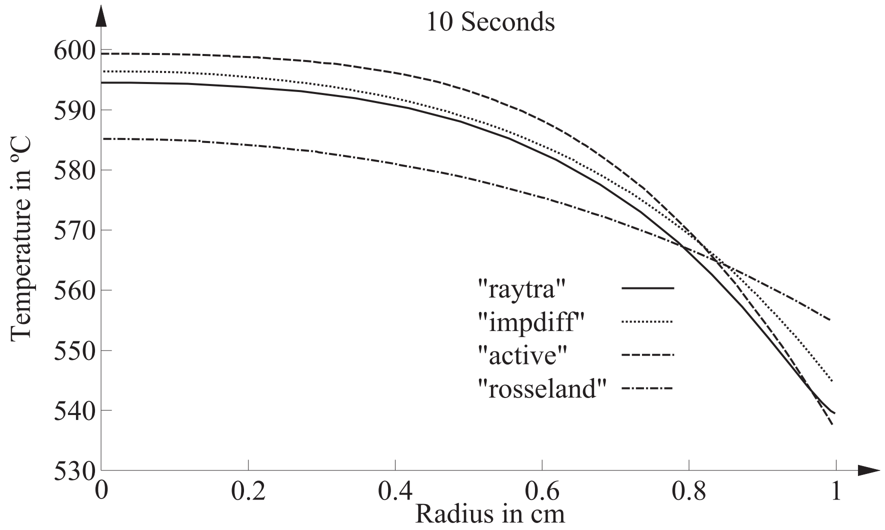

Figure 9. Comparison between the temperature profiles calculated by different approximation methods.

The temperature calculated by the ray-tracing and the hybrid method is plotted in figure 10. The interface for the hybrid method is located of 0.2 cm away from the boundary. The difference between the temperature profiles is less than 4°C. The CPU time for the solution with the hybrid method is about 3 times smaller than the ray-tracing.

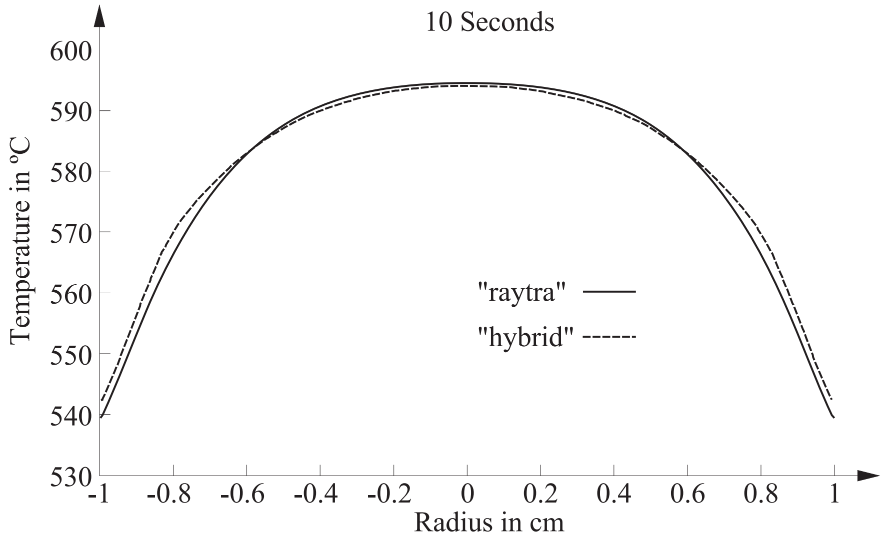

Figure 10. Comparison between the temperatures calculated by the ray-tracing and the hybrid method after 10 seconds.

6 Conclusion

Both efficient and sufficiently accurate algorithms for solving the 3D radiative heat transfer equation within semitransparent media are required to tackle the real cooling behavior of semitransparent materials. Although there is a continuous increase in computer power, efficient algorithms are extremely important to handle such cases in sufficient small times on workstations.

It was shown that in the temperature region $\leq 600°C$ the improved diffusion approximation is both efficient and sufficiently accurate. The easy implementation into commercial computer programs is an additional advantage in terms of usability.

The 'exact' solutions by ray-tracing or the discrete ordinates method will continue to serve as benchmark programs to determine the level of accuracy of the present and other approximate solution algorithms.

7 Symbols

A	symmetric diffusion tensor in form of a 3×3-matrix
a_j	element of the diffusion tensor
B	blackbody intensity (Planck function), $[\mathrm{Jm}^{-2}]$
c_0	velocity of light in vacuum, $= 2.9979 \times 10^8\,\mathrm{ms}^{-1}$
c_m	specific heat at constant pressure, $[\mathrm{J\,kg}^{-1}\mathrm{K}^{-1}]$
d	distance, [m]
G	integration domain
h	convective heat transfer coefficient, $[\mathrm{Wm}^{-2}\mathrm{K}^{-1}]$
h_p	Planck's constant, $= 6.6262 \times 10^{-34}\,\mathrm{Js}$
I	radiative intensity, $[\mathrm{Jm}^{-2}]$
k_h	thermal conductivity, $[\mathrm{Wm}^{-1}\mathrm{K}^{-1}]$
k_B	Boltzmann's constant, $= 1.3806 \times 10^{-23}\mathrm{JK}^{-1}$
M_k	number of spectral bands
$\vec{n} = (n_x, n_y, n_z)^T$	outer normal vector
n_g	refractive index of glass, =1.46
$\vec{q}$	radiative heat flux vector, $[\mathrm{Jm}^{-2}]$
$\vec{r} = (x, y, z)$	position vector, [m]
$\vec{r}_g = (x_g, y_g, z_g)$	position vector of a boundary point, [m]
S^2	unit sphere
s	path along a direction, [m]
t	time, [s]
T	absolute temperature, [K]
T_a	temperature of the surrounding, [K]
T_0	initial temperature, [K]
W_r	radiant energy, $[\mathrm{Jm}^{-3}]$

W_{emis}	radiant energy due to emission, [Jm^{-3}]
W_{absorp}	radiant energy due to absorption, [Jm^{-3}]
∂G	boundary of the integration domain
ε	mean hemispheric surface emissivity in the opaque spectral region, =0.9
$\kappa(\nu)$	extinction coefficient, [m^{-1}]
κ_k	extinction coefficient of the k-th spectral band, [m^{-1}]
$\bar{\kappa}_{Ross}$	Rosseland mean extinction coefficient, [m^{-1}]
λ	wavelength, [m]
ν	frequency, [s^{-1}]
ρ_m	density, [kgm^{-3}]
ρ	reflectivity
σ	Stefan-Boltzmann constant $= 5.670 \times 10^{-8}\,\mathrm{Wm}^{-2}\mathrm{K}^{-4}$
$\vec{\Omega} = (\Omega_1, \Omega_2, \Omega_3)^T$	angular direction vector
$\vec{\nabla} = \left(\frac{\partial}{\partial x}, \frac{\partial}{\partial y}, \frac{\partial}{\partial z}\right)^T$	Nabla operator

Acknowledgment

This work was done by a cooperation between Schott Glaswerke Mainz (Germany) and Institut für Techno- und Wirtschaftsmathematik e.V. Kaiserslautern (Germany) and was supported by a grant from the "Stiftung Rheinland-Pfalz für Innovation" (Rheinland Pfalz, Germany).

References

[1] Pan Y.H., Aung W., Reiss R.: Diffusion approximations for interaction of radiation and conduction in fused silica. 1989 National Heat Transfer Conference, HTD-Vol.106. Heat Transfer Phenomena in Radiation, Combustion and Fires.

[2] Modest M.F.: Radiative heat transfer. McGraw-Hill Inc., 1993.

[3] Siegel R., Howell J.R.: Thermal radiation heat transfer. Hemisphere Publishing Corporation, 1992.

[4] Viskanta R., Anderson E.E.: Heat tranfer in semitransparent solids. Advances in Heat Transfer, Vol.11 (1975), p.318-441.

[5] Fiveland W.A.: Discrete ordinate methods for radiative heat transfer in isotropically and anisotropically scattering media. ASME Journal of Heat Transfer, Vol.109 (1987), p.809-812.

[6] Truelove J.S.: Discrete-ordinate solutions of the radiation transport equation. ASME Journal of Heat Transfer, vol.109, No.4 (1987), p.1048-1051.

[7] Fiveland W.A.: The selection of discrete ordinate quadrature sets for anisotropic scattering. Fundamentals of Radiative Heat Transfer, ASME (1991), p. 89-96.

[8] Koch R., Krebs W., Wittig S., Viskanta R.: Discrete ordinates quadrature schemes for multidimensional radiative transfer. J. Quant. Spectrosc. Radiat. Transfer Vol.53, No.4 (1995), p. 353-372 .

[9] Rosseland S.: Note on the absorption of radiation within a star. M.N.R.A.S. 84 (1924), p. 525.

[10] Fotheringham U., Lentes F.-T.: Active thermal conductivity of hot glass. Glastech. Ber. Glass Sci. Technol. 67 No. 12(1994),p. 335-342.

[11] Arpaci V.S., Larsen P.S.: A thick gas model near boundaries. AIAA Journal, Vol.7, No.4 (1969), p.602-606.

[12] Fiveland W.A., Jessee J.P.: A finite element formulation of the discrete-ordinates method for multidimensional geometries. HTD-Vol.244, Radiative Heat Transfer: Theory and Applications, ASME (1993), p.41-48.

[13] Glatt L., Olfe D.B.: Radiative equilibrium of a gray medium in a rectangular enclosure. Journal of Quantitative Spectroscopy and Radiative Transfer, Vol.13 (1973), p.881-895.

[14] Howell J.R.: Thermal radiation in participating media: the past, the present, and some possible futures. Transactions of the ASME, Vol.110 (1988), p.1220-1229.

[15] Modest M.F.: Two-dimensional radiative equilibrium of a gray medium in a plane layer bounded by gray nonisothermal walls. ASME Journal of heat transfer, Vol.96C (1974), p.483-488.